




Cutting Force and Cutting Temperature Prediction in Drilling Using Finite Element Analysis

Tran Vu Minh ¹, Dinh Thi Phuong Thao ¹, Nguyen Xuan Luu ¹, Nguyen Thi Anh ²,
and Tran Thanh Tung ^{3,*}

¹ School of Mechanical Engineering, Ha Noi University of Science and Technology, Ha Noi, Vietnam

² Faculty of Mechanical Engineering, Thuyloi University, Ha Noi, Vietnam

³ Faculty of Engineering Mechanics and Automation, VNU University of Engineering and Technology, Ha Noi, Vietnam

Email: minh.tranvu@hust.edu.vn (T.V.M.); thao.dtp232315m@sis.hust.edu.vn (D.T.P.T.);

luu.nx240218e@sis.hust.edu.vn (N.X.L.); nguyenthianh200197@tlu.edu.vn (N.T.A.);

tranthanh tung@vnu.edu.vn (T.T.T.)

*Corresponding author

Abstract—Drilling is a crucial metal cutting operation extensively employed in the mechanical engineering sector. Predicting the temperature and cutting forces (forces and torques) occurring during drilling on any material and affecting the drill bit will play a positive role in estimating the life of the drill bit and thus achieving better hole quality and accuracy. In this study, drilling force and temperature were studied during Aluminum drilling using finite element method as an alternative to experimental. This topic aims to determine the cutting force and temperature in the cutting zone by analyzing the input parameters of cutting speed and feed rate during the simulation of a high-speed steel drill bit on AL 7075-T6 material. This paper introduces a methodology for developing two finite element models: the Finite Element Method (FEM) and Smoothed Particle Hydrodynamics (SPH) for drilling simulation. The simulations are performed using the LSDYNA code based on available real experiments. The accuracy of the model makes it a satisfactory approach for drilling experiments. The two presented models can verify the drilling process and predict the heat and cutting forces occurring during drilling operation.

Keywords—Finite Element Method (FEM), Drilling, Cutting force, Finite Element Analysis (FEA), Smoothed Particle Hydrodynamics (SPH) model

I. INTRODUCTION

Drilling is a crucial metal cutting operation extensively employed in the mechanical engineering sector. Despite advancements in modern machining techniques within the manufacturing sector, conventional drilling remains the predominant method due to its cost-effectiveness and simplicity [1–5]. Cutting parameters (cutting speed, cutting depth, and feed rate) are the paramount factors in the drilling process, influencing its efficiency and directly

impacting the temperature and cutting force in the cutting zone [6–12]. During the machining process, the cutting tool performs the cutting process in a very difficult environment, where high contact stress [13–16] and high temperature spread, so wear is inevitable [17–20].

Predicting the temperature and cutting forces (forces and torques) occurring during drilling on any material and affecting the drill bit will play a positive role in estimating the life of the drill bit and thus achieving better hole quality and accuracy. Moreover, the predicted life of the drill bit will increase the product quality and reduce production cost. To determine the cutting load (forces and torques) and cutting temperature, there are two methods: experimental [21–25] and simulation [26–32]. Experimental drilling methods are being extensively studied to improve efficiency, safety, and effectiveness across different types of drilling operations. However, the experimental method is costly and time-consuming.

In this study, drilling force and temperature were studied during Aluminum drilling using finite element method as an alternative to experimental. This topic's goal is to simulate an HSS drill bit on AL 7075-T6 material and use the input parameters of cutting speed and feed rate to calculate the cutting force and cutting zone temperature. Next, contrast the outcomes with those of the experiment. Because simulation results agree with experiments, finite element simulation is a useful tool for studying the drilling process.

II. LITERATURE REVIEW

Moreover, the advancement of computer technology has led to the widespread utilization of simulation methods employing software like Ls Dyna to mitigate the drawbacks of experimental approaches. The

forementioned software utilizes the Finite Element Method (FEM). The Finite element Method (FEM) is an approximate technique for addressing metal cutting issues. The solution of the problem is obtained based on solving the equilibrium equation of the entire computational domain according to the principle of extreme equilibrium. Typically, there are two primary methods for simulating the drilling process: Finite Element Method (FEM) and Smoothed Particle Hydrodynamics (SPH).

Finite Element Method (FEM) is employed when a three-dimensional model is necessary to depict the tool's geometry and the extent of material deformation [33–37]. The FEM method with dynamic re-meshing is expected to provide the most accurate predictions of cutting force and cutting temperature.

SPH is a conventional mathematical method utilized to address drilling issues. In contrast to numerical methods, Smoothed Particle Hydrodynamics (SPH) is a mesh-free, Lagrangian approach that does not necessitate a mesh for materials [38–42]. The developed SPH model demonstrates its capacity to account for continuous and shear localized chip formation while accurately estimating the cutting forces, as evidenced in drilling. The SPH model is employed to enhance the comprehension of machining with worn tools.

III. MATERIALS AND METHODS

A. Finite Element of Drill Simulation Impact Test

A drill bit is a tool that enables a drill to create holes in diverse materials by applying circular torque or rotational force. Fig. 1 displays the characteristics of the drill bit utilized in the research. The drill bit has an overall length of 117 mm, a flute length of 95 mm, a drill diameter of 8 mm, and a point angle of 140°.

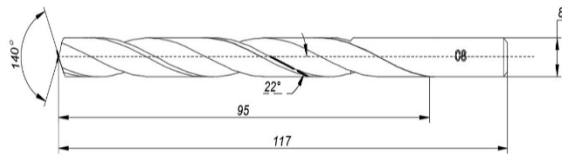


Fig. 1. Drill geometry parameter.

The drill bit is easily affected by the force when used. For ease of analysis, it can be separated into the tangential component P_z , the radial component P_y and the axial component P_x . When drilling, the forward force is denoted by P_x . The axial force P_x can be calculated by some empirical formulas.

$$P_x = 0.195HBS^{0.8}d^{0.8} + 0.0022HBd^2 \quad (1)$$

The Torque P_z can be calculated as follow:

$$P_z = Cd^2S^{0.8}HB^{0.7} \quad (2)$$

where: HB is Brinell hardness
 S is Cutting speed (RPM).

d is denoted the diameter of drill tool (mm).
 C is coefficient and $C = 2.10^6$

The numerical simulations were carried out using LS-DYNA, a commercial finite element code well-suited for high-speed machining and impact simulations. LS-DYNA offers extensive support for Lagrangian solid elements, Smoothed Particle Hydrodynamics (SPH), and rigid body modeling, making it an effective tool for capturing the complex thermo-mechanical behavior of the cutting process. Its capabilities to simulate large plastic deformation, material separation, and tool-workpiece interaction allow for realistic modeling of chip formation and stress evolution during milling operations. The software's wide range of material models (e.g., Johnson-Cook with damage) and contact algorithms (e.g., eroding and automatic surface-to-surface) were essential for achieving accurate results in this study. Developing the accurate geometry of the tool and drill bit was an important step for the finite element simulation of the drilling operation. The model consists of a 15mm height, 10mm radius cylinder drilled with an HSS twist drill, as shown in Fig. 2. In the computer simulation, the workpiece is constrained in all directions. The drill simultaneously revolves about the Z axis and moves along the Z axis.

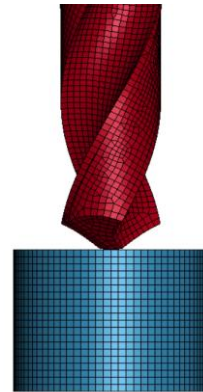


Fig. 2. Finite element of drilling simulation test.

The experiment was carried out with the following cutting conditions: cutting speed $V_c = 60$ m/min at feed rate $f_z = 0.05, 0.1, 0.2$ mm/rev, respectively. The cutting tool is less deformed than the workpiece. Usually for heat and force simulation problems, the cutting tool is considered as rigid. SPH is best suited for modeling highly deformable, fragmenting, or eroding materials, which is unnecessary for a rigid tool. SPH is not suitable for the cutting tool, where precise geometry, contact, and low deformation are key—FEM (especially rigid elements) is a more efficient and accurate choice. The maximum mesh size is 0.5 mm, the minimum size is 0.01 mm, the arbitrary geometry results in 23,436 elements for the drill bit as shown in Fig. 3. Tungsten carbide-cobalt (WC-Co) is a composite material commonly used in cutting tools due to its high hardness, wear resistance, and thermal stability. In LS-DYNA, WC-Co is typically modeled as a rigid material when tool deformation is negligible, or as an elastic/plastic material with failure when studying tool wear or impact. For most machining simulations where the

tool does not deform significantly, use *MAT_020 (Rigid)* for WC-Co.



Fig. 3. Finite element of drill tool.

Both SPH and FEM are valuable tools for modeling workpieces in milling simulations. SPH excels in simulating chip formation, material failure, and extreme deformations, while FEM provides high accuracy for stress distribution, thermal analysis, and moderate deformations. A hybrid model is often the best solution when both chip formation and bulk material behavior need to be captured accurately. The FEM model consists of 47,961 nodes and 28,800 solid elements. The SPH model consists of 12,225 nodes as shown in Fig. 4. Each particle carries properties such as mass, position, velocity, density, and pressure. These nodes collectively approximate the physical behavior of the modeled material.

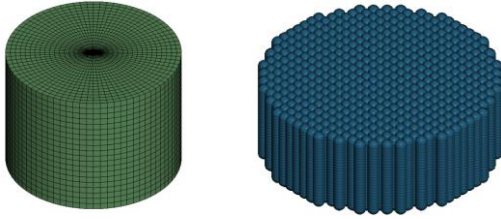


Fig. 4. Workpiece modelling: FEM (left) and SPH (right) model.

Material type 15 applies to the high-rate deformation of various materials, including the majority of metals. The material properties' of model used in this study are given in Table I. Johnson and Cook express the flow stress as:

$$\sigma_y = (A + B\varepsilon^n)(1 + C\ln\varepsilon^*)(1 - T^m) \quad (3)$$

In this equation, A , B , C , m and n are input constants T represents the homologous temperature, ε and ε^* are effective plastic strain. A represents yield strength measured in megapascals (MPa). B represents the hardening modulus (MPa), n denotes the strain hardening exponent, C signifies the strain rate sensitivity coefficient, and m indicates the thermal softening exponent.

TABLE I. PARAMETERS OF THE JOHNSON-COOK MODEL

Parameter	A	B	C	m	n	T^m
Unit	GPa	GPa	-	-	-	°C
Value	0.546	0.678	0.024	1.56	0.71	635

EOS-POLYNOMIAL were used, the linear polynomial equation of state is linear in internal energy, the pressure is given by

$$P = C_0 + C_1\mu + C_2\mu_2 + C_3\mu_3 + (C_4 + C_5\mu + C_6\mu_2)E \quad (4)$$

In which: E is the units of pressure, C_i is the i th polynomial equation coefficient. In practical drilling scenarios, the tool's deformation regarding the material is

not significant, and tool wear is insignificant. Consequently, the drill bit is classified as a rigid body within the contact module, as shown in Table II.

TABLE II. MATERIAL PROPERTIES OF DRILL TOOL AND WORKPIECE

Parameter	Al 7075-T6	Steel
Density (kg/mm ³)	2.81e-06	7.85e-06
Young modulus (GPa)	71.7	200
Poisson ratio	0.33	0.3

IV. RESULT AND DISCUSSION

Fig. 5 shows the results of the drilling simulation including both FEM and SPH methods. The simulation results align well with experimental observations, demonstrating that the model accurately predicts physical behavior during drilling. This validation improves the belief in the model's dependability. To validate the accuracy of the FE model, a comparison between experimental results in [33] and simulation findings will be conducted in the following two parameters: force and temperature.

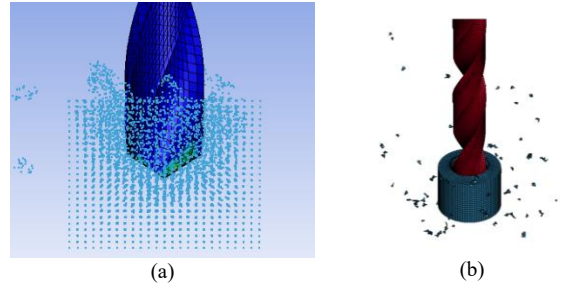


Fig. 5. Drill simulation results with (a) SPH model and (b) FEM model.

Figs. 6 and 7 show the temperature simulation results at 3 points at the drill tip P1, P2, P3 (in case of using SPH) and Q1, Q2, Q3 (in case of using FEM).

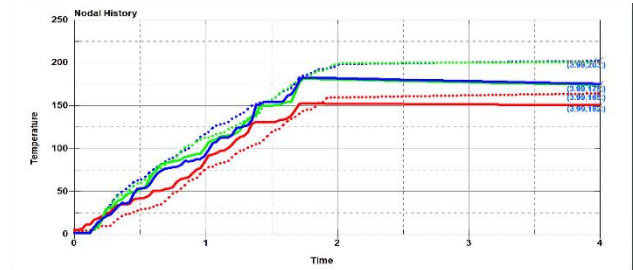


Fig. 6. Temperature at 6 points P1, P2, P3, Q1, Q2, Q3.

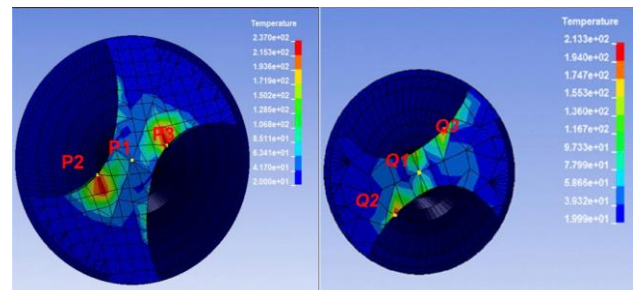


Fig. 7. Three points on the drill head SPH (left), FEM (right).

The results show that the temperature when simulated by SPH at 2 points P1 and P2 is always higher than the corresponding 2 points Q1 and Q2 when simulated by FEM. Meanwhile, at point P3, the temperature is lower when simulated by SPH at temperatures below 1500 C, and higher when the temperature is from 150 to 2000 C compared to the corresponding point Q3 in FEM.

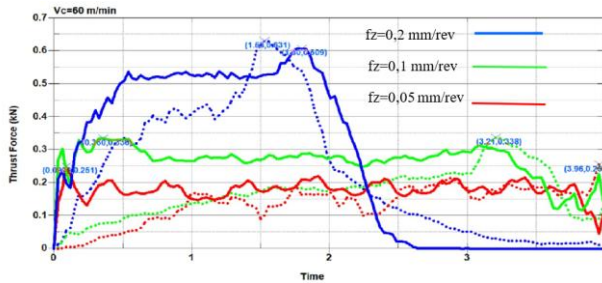


Fig. 9. Force diagram at cutting speed $V_c = 60$ m/min.

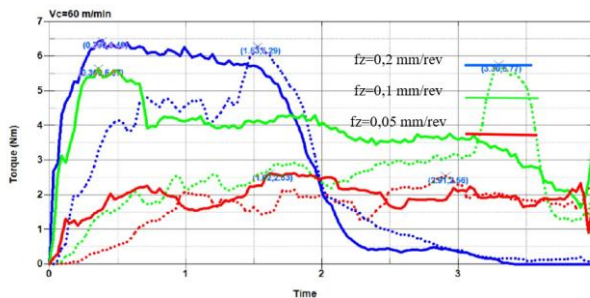


Fig. 10. Torque diagram at cutting speed $V_c = 60$ m/min.

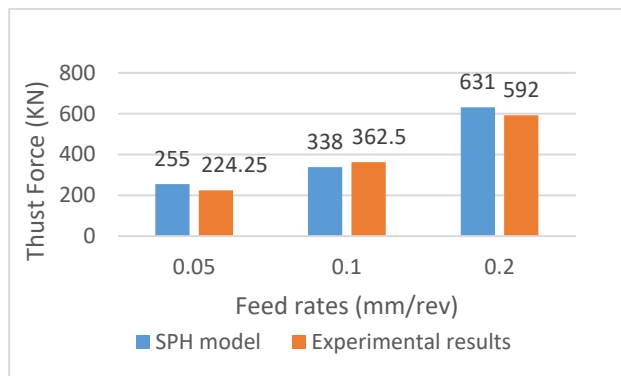


Fig. 11. Comparison of forces from experimental results [33] and SPH simulation.

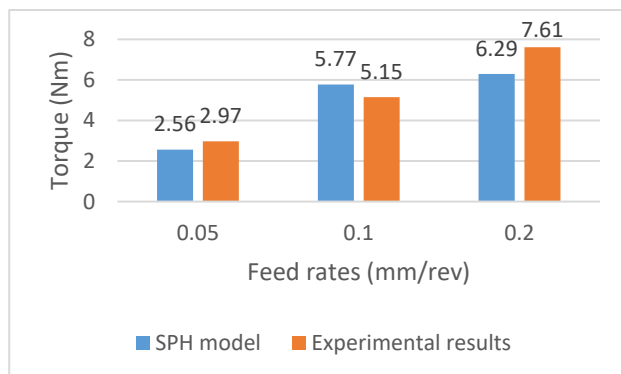


Fig. 12. Comparison of torque from experimental results [33] and SPH model simulation.

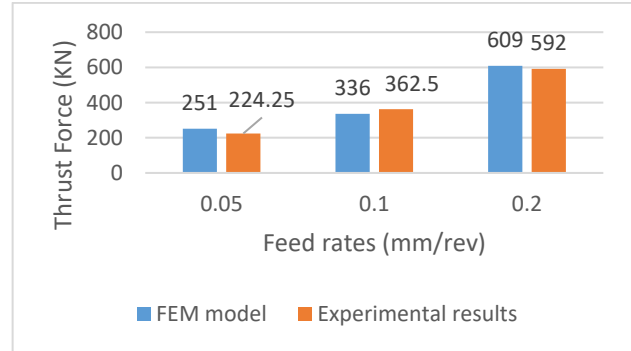


Fig. 13. Comparison of forces from experimental results [33] and FEM simulation.

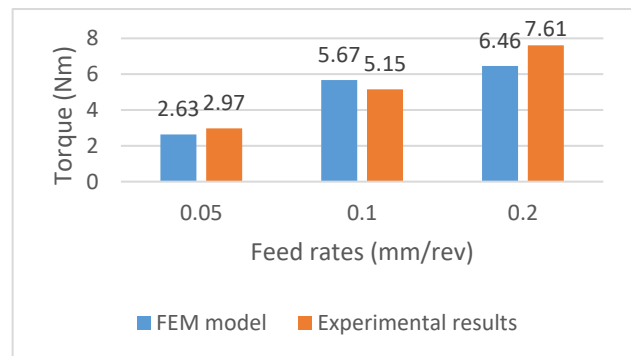


Fig. 14. Comparison of torque from experimental results [33] and FEM simulation.

The results of both FEM and SPH models in the Figs. 9–14 show that the drilling temperature increases as the feed rate increases, when increasing the feed rate from $f_z = 0.05$ mm/rev to $f_z = 0.1$ mm/rev at the main cutting speed $V_c = 60$ m/min, with the SPH model at 2.49 s the drilling temperature increases from 179 °C to 199 °C. Increasing the feed rate to $f_z = 0.2$ mm/rev will increase the temperature up to 231 °C. In the FEM model when $f_z = 0.05$ mm/rev the temperature is 147 °C, 177 °C at $f_z = 0.01$ mm/rev and reaches 204 °C when $f_z = 0.2$ mm/rev.

Regarding the thrust force criterion, the SPH model's error in percentage is: 13.7%, 7.24%, 6.58% corresponding to the feed rates of $f_z = 0.05$ mm/rev, $f_z = 0.1$ mm/rev, $f_z = 0.2$ mm/rev, respectively. As for the FEM model, the error is 11.92%, 7.31%, 2.87% corresponding to the feed rates of $f_z = 0.05$ mm/rev, $f_z = 0.1$ mm/rev, $f_z = 0.2$ mm/rev, respectively.

The torque in the FEM model has an error of <20%. When $f_z = 0.05$ mm/rev, the simulation value is 2.63 Nm, while the experimental value is 2.87 Nm, with an error of 8.36%. In the case of $f_z = 0.1$ mm/rev, the error is 11.17%, and the remaining error is 15.11% when $f_z = 0.2$ mm/rev. Looking at the chart, we can see the increasing trend of torque when increasing f_z . Similarly, the SPH model has errors of 10.8%, 13.13%, 17.34%, respectively. The explanation for this is that when the feed rate increases, it means that the drill bit thrust increases, cutting and breaking more material in each revolution. According to formula $M = F \times r$, the thrust F increases, the torque also increases with the rotating arm r remaining constant. Table III is a summary of the simulation results.

TABLE III. SIMULATION RESULTS IN SPH AND FEM MODELS

Items	V_c (m/min)	f_z (mm/rev)	SPH Model	FEM Model	Experimenta l results [33]	Difference relative (SPH)	Difference relative (FEM)
Temperature	60	0.2	231	204	-----	-----	-----
		0.1	199	177	-----	-----	-----
		0.05	179	147	-----	-----	-----
Force (N)	60	0.2	631	609	592	6.58%	2.87%
		0.1	338	336	362.5	7.24%	7.31%
		0.05	255	251	224.25	13.7%	11.92%
Torque (Nm)	60	0.2	6.29	6.46	7.61	17.34%	15.11%
		0.1	5.77	5.67	5.15	12%	10.1 %
		0.05	2.56	2.63	2.97	13.8%	11.4 %
Simulation time	60	0.2	2 h & 15 s	5 h & 38 s	-----		
		0.1	2 h & 15 s	5 h & 38 s	-----		
		0.05	2 h & 15 s	5 h & 38 s	-----		

There is a certain error between simulation and experiment, reasons for Deviations in Cutting Force and Heat Between Experiment and LS-DYNA Simulation. Tool and workpiece are often simplified: Tool is modeled as rigid, idealized geometry (no coatings or wear), Initial workpiece temperature is constant (ignores pre-heating or cutting environment). In milling, tool-chip contact is dynamic, with high-pressure and micro-slip behavior. LS-DYNA uses Coulomb friction (constant coefficient), which doesn't capture: variable friction due to surface oxidation, temperature, or wear and sticking and sliding zones along the rake face

The temperature in both models increases as the feed rate increases. The explanation for this phenomenon may be that the chip thickness and friction increase as the feed rate increases. As the feed rate increases, the chip becomes thicker, which means that the ratio of surface area to chip thickness decreases. As the surface area decreases, the heat dissipation capacity also decreases. Therefore, the heat generated by friction cannot be dissipated quickly, resulting in an increase in temperature. The tool temperature is monitored while rotating at a speed of $V_c = 60$ m/min and a feed rate of $f_z = 0.1$ mm/rev. The purpose of this study is to study the temperature distribution and variation on the surface of the drill bit during drilling. Only representative grains are selected for study and not too many points are selected. As shown in Fig. 7 three points are marked on the edge of the drill.

P1(SPH), Q1(FEM) are placed in the middle of the chisel edge of the drill bit P2, P3 and Q2, Q3 are placed on the two edges of the main drill bit. The temperature changes of these points are monitored. As shown in the temperature curve, the temperature increases rapidly in the initial plunge stage and the temperature change at steady state is relatively small. The temperatures at P2, P3 and Q2, Q3 are similar and the change trend is similar. The temperatures at P1 and Q1 are slightly lower than those at the main drill edge because the main drilling operation does not take place at P1, Q1 and it takes place at P2, P3 and Q2, Q3. P1, Q1 heat is mainly generated by friction, so the temperature increase due to drilling at the remaining points is more obvious. This is also consistent with the actual situation, consistent with the distribution and change law of temperature on the surface during drilling.

V. CONCLUSION

This paper presents a method for constructing two finite element models (FEM and SPH) for drilling modeling. The simulations are performed using the LSDYNA code based on available real experimental results. The accuracy of the model makes it a satisfactory approach for drilling experiments. The two presented models can verify the drilling process and predict the heat and cutting forces occurring during drilling operation. Regarding the thrust force criterion, the SPH model's error in percentage is: 13.7%, 7.24%, 6.58% corresponding to the feed rates of $f_z = 0.05$ mm/rev, $f_z = 0.1$ mm/rev, $f_z = 0.2$ mm/rev respectively. As for the FEM model, the error is 11.92%, 7.31%, 2.87% corresponding to the feed rates of $f_z = 0.05$ mm/rev, $f_z = 0.1$ mm/rev, $f_z = 0.2$ mm/rev respectively.

The torque in the FEM model has an error of <20%. When $f_z = 0.05$ mm/rev, the simulation value is 2.63 Nm, while the experimental value is 2.87 Nm, with an error of 8.36%. In the case of $f_z = 0.1$ mm/rev, the error is 11.17%, and the remaining error is 15.11% when $f_z = 0.2$ mm/rev. Looking at the chart, we can see the increasing trend of torque when increasing f_z . Similarly, the SPH model has errors of 10.8%, 13.13%, 17.34%, respectively

Additionally, the findings show that drilling can be studied using computers rather than costly experimental testing. The proposed model can be used as a reliable tool to support the investigation and development of optimization for future drilling processes. The results shown that Smoothed Particle Hydrodynamics (SPH) is the preferred method for cutting force, severe deformation, and high strain rate conditions in milling. In contrast, Finite Element Method (FEM) is better suited for thermal behavior, chip separation in simulation. Future work should focus on: Enhancing hybrid FEM-SPH coupling techniques to leverage the strengths of both methods

CONFLICT OF INTEREST

The authors declare no conflict of interest.

AUTHOR CONTRIBUTIONS

Tran Vu Minh: Writing, Software, Original draft preparation, Investigation; Dinh Thi Phuong Thao:

Experiment, Design, Software, Simulation; Nguyen Xuan Luu: Design, Software, Simulation; Nguyen Thi Anh: Methodology, experiment; Tran Thanh Tung: Conceptualization, Methodology, Supervision, Reviewing and Editing. All authors had approved the final version.

FUNDING

This research is funded by the Hanoi University of Science and Technology (HUST) under project number T2024-PC-034.

REFERENCES

- [1] F. Ficici, "Investigation of wear mechanism in drilling of PPA composites for automotive industry," *J. Eng. Res.*, vol. 11, no. 2, 100034, 2023. doi: 10.1016/j.jer.2023.100034
- [2] M. Tolouei-Rad and M. Aamir, "Analysis of the performance of drilling operations for improving productivity," *Drilling Technology*, 2021, pp. 5–20. doi: 10.5772/intechopen.96497
- [3] C. Devitte *et al.*, "Optimization for drilling process of metal-composite aeronautical structures," *Sci. Eng. Compos. Mater.*, vol. 28, no. 1, pp. 264–275, 2021. doi: 10.1515/secm-2021-0027
- [4] M. Aamir *et al.*, "A review: Drilling performance and hole quality of aluminium alloys for aerospace applications," *J. Mater. Res. Technol.*, vol. 9, no. 6, pp. 12484–12500, 2020. doi: 10.1016/j.jmrt.2020.09.003
- [5] J. B. Chandar, L. Nagarajan, and M. S. Kumar, "Recent research progress in deep hole drilling process: A review," *Surf. Rev. Lett.*, vol. 28, no. 11, 2130003, 2021. doi: 10.1142/S0218625X21300033
- [6] M. Aamir *et al.*, "Effect of cutting parameters and tool geometry on the performance analysis of one-shot drilling process of AA2024-T3," *Metals*, vol. 11, no. 6, 854, 2021. doi: 10.3390/met11060854
- [7] I. Boughdiri *et al.*, "Effect of cutting parameters on thrust force, torque, hole quality and dust generation during drilling of GLARE 2B laminates," *Compos. Struct.*, vol. 261, 113562, 2021. doi: 10.1016/j.compstruct.2021.113562
- [8] S. Strodick *et al.*, "Influence of cutting parameters on the formation of white etching layers in BTA deep hole drilling," *TM-Tech. Mess.*, vol. 87, no. 11, pp. 674–682, 2020. doi: 10.1515/teme-2020-0046
- [9] J. Xu *et al.*, "A review on CFRP drilling: Fundamental mechanisms, damage issues, and approaches toward high-quality drilling," *J. Mater. Res. Technol.*, vol. 24, pp. 9677–9707, 2023. doi: 10.1016/j.jmrt.2023.05.023
- [10] B. Ozdemir *et al.*, "Optimization of parameters for drilling composite materials with freeform surfaces," *Mater. Manuf. Process.*, vol. 39, no. 1, pp. 55–68, 2024. doi: 10.1080/10426914.2023.2187826
- [11] Y. Fedai, "Optimization of drilling parameters in drilling of MWCNT-reinforced GFRP nanocomposites using fuzzy AHP-weighted Taguchi-based MCDM methods," *Processes*, vol. 11, no. 10, 2872, 2023. doi: 10.3390/pr11102872
- [12] H. Tian *et al.*, "Influence of drilling parameters on bone drilling force and temperature by FE simulation and parameters optimization-based Taguchi method," *Alex. Eng. J.*, vol. 75, pp. 115–126, 2023. doi: 10.1016/j.aej.2023.05.048
- [13] T. Gao *et al.*, "Carbon fiber reinforced polymer in drilling: From damage mechanisms to suppression," *Compos. Struct.*, vol. 286, 115232, 2022. doi: 10.1016/j.compstruct.2022.115232
- [14] C. G. Yuan *et al.*, "Drilling of titanium alloy (Ti6Al4V)—A review," *Mach. Sci. Technol.*, vol. 25, no. 4, pp. 637–702, 2021. doi: 10.1080/10910344.2021.1925295
- [15] Y. Liu, L. He, and S. Yuan, "Wear properties of aluminum alloy 211z.1 drilling tool," *Jordan J. Mech. Ind. Eng.*, vol. 15, no. 1, 2021.
- [16] Y. Liu *et al.*, "A study on strengthening and machining integrated ultrasonic peening drilling of Ti-6Al-4V," *Mater. Des.*, vol. 212, 110238, 2021. doi: 10.1016/j.matdes.2021.110238
- [17] D. Xiao *et al.*, "Research on wellbore temperature control and heat extraction methods while drilling in high-temperature wells," *J. Pet. Sci. Eng.*, vol. 209, 109814, 2022. doi: 10.1016/j.petrol.2021.109814
- [18] Z. Zhang *et al.*, "Effect of the variations of thermophysical properties of drilling fluids with temperature on wellbore temperature calculation during drilling," *Energy*, vol. 214, 119055, 2021. doi: 10.1016/j.energy.2020.119055
- [19] A. K. Sahoo *et al.*, "Parametric optimization of CNC-drilling of Inconel 718 with cryogenically treated drill-bit using Taguchi-Whale optimization algorithm," *Mater. Today Proc.*, vol. 50, pp. 1591–1598, 2022. doi: 10.1016/j.matpr.2021.09.121
- [20] H. KB *et al.*, "Effects of machining parameters on H13 die steel using CNC drilling machine," *Compos. Adv. Mater.*, vol. 32, 26349833231189296, 2023. doi: 10.1177/26349833231189296
- [21] H. Gökçe, "Modelling and optimization for thrust force, temperature and burr height in drilling of custom 450," *Exp. Tech.*, vol. 46, no. 4, pp. 707–721, 2022. doi: 10.1007/s40799-021-00510-z
- [22] C. T. Xiang *et al.*, "Investigating twist drill design influence on thrust force and surface roughness in drilling AFRP/Al7075-T6 stacks materials," *Int. J. Nanoelectron. Mater.*, vol. 17, pp. 251–256, 2024. doi: 10.58915/ijneam.v17iJune.865
- [23] A. Sharma *et al.*, "Influence of cutting force and drilling temperature on glass hole surface integrity during rotary ultrasonic drilling," in *Adv. Prod. Ind. Eng.*, Springer, 2021, pp. 369–378. doi: 10.1007/978-981-15-5519-0_28
- [24] P. Kyratsis, A. Tzotzis, and J. P. Davim, "Experimental and 3D numerical study of AA7075-T6 drilling process," in *3D FEA Simulations in Machining*, Springer, 2023, pp. 63–75. doi: 10.1007/978-3-031-24038-6_4
- [25] W. Geng *et al.*, "Prediction model optimization and experimental verification based on the material characteristic and dynamic angle on thrust force and torque in drilling gjv450," *Int. J. Adv. Manuf. Technol.*, vol. 126, no. 11, pp. 5571–5582, 2023. doi: 10.1007/s00170-023-11452-8
- [26] M. S. Abd-Elwahed *et al.*, "Experimental and numerical FEM of woven GFRP composites during drilling," *Struct. Eng. Mech.*, vol. 80, no. 5, pp. 503–522, 2021. doi: 10.12989/sem.2021.80.5.503
- [27] Y. Kaplan and M. Nalbant, "Experimental and numerical investigation of the thrust force and temperature generation during a drilling process," *Mater. Test.*, vol. 63, no. 6, pp. 581–588, 2021. doi: 10.1515/mt-2020-0097
- [28] A. Tzotzis *et al.*, "FEM based investigation on thrust force and torque during Al7075-T6 drilling," in *IOP Conf. Ser. Mater. Sci. Eng.*, vol. 1037, no. 1, 012009, 2021. doi: 10.1088/1757-899X/1037/1/012009
- [29] P. Kyratsis, A. Tzotzis, and J. P. Davim. (2023). *3D FEA Simulations in Machining*. Springer. [Online]. Available: <https://link.springer.com/book/10.1007/978-3-031-24038-6>
- [30] T. T. Tung, N. Y. Nhi, and N. T. Anh. (2021). A study on simulation of metal cutting process based on Ls-Dyna," *J. Tech. Univ. Gabrovo*. [Online]. 62. pp. 47–55. Available: <http://izvestia.tugab.bg/index.php?m=27&id=296>
- [31] J. Priest *et al.*, "3D finite element modelling of drilling: The effect of modelling method," *CIRP J. Manuf. Sci. Technol.*, vol. 35, pp. 158–168, 2021. doi: 10.1016/j.cirpj.2021.06.001
- [32] P. Hale and E. G. Ng, "3D finite element model on drilling of CFRP with numerical optimization and experimental validation," *Materials*, vol. 14, no. 5, 1161, 2021. doi: 10.3390/ma14051161
- [33] I. Ucu, "3D finite element modelling of drilling process of Al7075-T6 alloy and experimental validation," *J. Mech. Sci. Technol.*, 2016. doi: 10.1007/s12206-016-0341-0
- [34] Y. Yang and J. Sun, "Finite element modelling and simulating of drilling of titanium alloy," in *Proc. 2009 Second Int. Conf. Inf. Comput. Sci.*, Manchester, UK, 2009, pp. 178–181. doi: 10.1016/j.proeng.2011.04.312
- [35] E. Oezkaya, S. Hannich, and D. Biermann, "Development of a three-dimensional finite element method simulation model to predict modified flow drilling tool performance," *Int. J. Mater. Form.*, vol. 12, pp. 477–490, 2019. doi: 10.1007/s12289-018-1429-0
- [36] B.-A. Behrens *et al.*, "Finite element and finite volume modelling of friction drilling HSLA steel under experimental comparison," *Materials*, vol. 14, no. 20, 5997, 2021. doi: 10.3390/ma14205997
- [37] S. Gholampour *et al.*, "Thermal and physical damage in skull base drilling using gas cooling modes: FEM simulation and experimental evaluation," *Comput. Methods Programs Biomed.*, vol. 212, 106463, 2021. doi: 10.1016/j.cmpb.2021.106463

- [38] T. A. Nguyen and T. T. Tran. (2020). Drilling modelling using computer simulation. *Int. J. Sci. Technol. Res.* [Online]. 9(10), pp. 171–174. Available: <https://www.ijstr.org/final-print/oct2020/Drilling-Modelling-Using-Computer-Simulation.pdf>
- [39] I. S. Boldyrev and D. I. Topolov, “Twist drilling SPH simulation for thrust force and torque prediction,” in *IOP Conf. Ser. Mater. Sci. Eng.*, vol. 971, no. 2, 022044, 2020. doi: 10.1088/1757-899X/971/2/022044
- [40] D. Shah and A. N. Volkov, “Simulations of deep drilling of metals by continuous wave lasers using combined smoothed particle hydrodynamics and ray-tracing methods,” *Appl. Phys. A*, vol. 126, no. 2, 82, 2020. doi: 10.1007/s00339-019-3202-8
- [41] A. Mardalizad *et al.*, “Numerical modeling of the tool-rock penetration process using FEM coupled with SPH technique,” *J. Pet. Sci. Eng.*, vol. 189, 107008, 2020. doi: 10.1016/j.petrol.2020.107008
- [42] A. Baumann *et al.*, “Cutting-fluid flow with chip evacuation during deep-hole drilling with twist drills,” *Eur. J. Mech. B Fluids*, vol. 89, pp. 473–484, 2021. doi: 10.1016/j.euromechflu.2021.07.003

Copyright © 2025 by the authors. This is an open access article distributed under the Creative Commons Attribution License which permits unrestricted use, distribution, and reproduction in any medium, provided the original work is properly cited ([CC BY 4.0](https://creativecommons.org/licenses/by/4.0/)).